A New One-Dimensional Platinum System Consisting of Carboxylate-Bridged *cis*-Diammineplatinum Dimers[1]

Ken Sakai,*,† Masao Takeshita,† Yuko Tanaka,† Takuma Ue,† Masayuki Yanagisawa,† Masaya Kosaka,† Taro Tsubomura,† Masamichi Ato,‡ and Takeo Nakano§

Contribution from the Department of Industrial Chemistry, Faculty of Engineering, Seikei University, Kichijoji-Kitamachi, Musashino, Tokyo 180-8633, Japan, Department of General Education, Senshu University, Higashi-Mita, Tama-ku, Kawasaki, Kanagawa 214-8580, Japan, and Department of Applied Physics, Seikei University, Kichijoji-Kitamachi, Musashino, Tokyo 180-8633, Japan

Received January 5, 1998

Abstract: With the aim of developing new 1D platinum chain solids having infinite Pt−Pt bonds, several carboxylate-bridged *cis*-diammineplatinum dimers have been prepared and structurally characterized. For a dimer doubly bridged with acetates, five different salts $[Pt_2(NH_3)_4(\mu\text{-}CH_3CO_2)_2]X_2\cdot nH_2O$ (X_2, $n = (ClO_4)_2$, 2, **1**; $(NO_3)_2$, 1, **2**; $(BF_4)_2$, 4, **3**; $(PF_6)_2$, 2, **4**; (SiF_6), 4, **5**) have been prepared. The crystal structure of **5** has revealed that an infinite dimer chain $[Pt_2(NH_3)_4(\mu\text{-}CH_3CO_2)_2]_n^{2n+}$ can be given as a result of hydrogen bond formation between the ammines and the oxygen atoms of acetates, demonstrating our prediction that the N_2O_2 coordination sphere may serve as a hydrogen-bonding moiety to assist formation of an infinite dimer chain. An asymmetric dimer bridged by both acetate and hydroxide ligands, $[Pt_2(NH_3)_4(\mu\text{-}CH_3CO_2)(\mu\text{-}OH)](SiF_6)$ (**6**), has also been isolated as a byproduct of **5**, and a similar 1D framework, $[Pt_2(NH_3)_4(\mu\text{-}CH_3CO_2)(\mu\text{-}OH)]_n^{2n+}$, has been characterized by X-ray diffraction. In addition, some glycolate-bridged analogues of similar frameworks have been synthesized and characterized: $[Pt_2(NH_3)_4(\mu\text{-}CH_2(OH)CO_2)_2](SiF_6)\cdot 4H_2O$ (**7**), $[Pt_2(NH_3)_4(\mu\text{-}CH_2(OH)CO_2)_2](ClO_4)_2\cdot H_2O$ (**8**), and $[Pt_2(NH_3)_4(\mu\text{-}CH_2(OH)CO_2)(\mu\text{-}OH)](NO_3)_2$ (**9**). To obtain partially oxidized systems, benzoate derivatives have been selected as bridging ligands. Although a benzoate system gave dark blue solids ascribable to mixed-valence Pt(2.25+) compounds, a crystallographically analyzed complex has turned out to be a double complex involving both a Pt(II) monomer and a dinuclear Pt(II) complex, $[Pt_2(NH_3)_4(\mu\text{-}C_6H_5CO_2)_2]_2(SiF_6)\ (BF_4)_2\cdot[cis\text{-}Pt(NH_3)_2(C_6H_5CO_2)_2]\cdot 3H_2O$ (**10**). Nevertheless, our final efforts in this work have revealed that a *p*-hydroxybenzoate system, $[Pt(2.25+)_2(NH_3)_4(\mu\text{-}p\text{-}C_6H_4(OH)CO_2)_2]_2X_5\cdot nH_2O$ (X_5, $n = (SO_4)_{2.25}(p\text{-}C_6H_4(OH)CO_2)_{0.5}$, 5, **12a**; $(PF_6)_2(SO_4)(p\text{-}C_6H_4(OH)CO_2)$, 6, **12b**; $(PF_6)_2(NO_3)_2(p\text{-}C_6H_4(OH)CO_2)$, 7, **12c**), may be suited to achieve a 1D platinum blue system. The compounds display a blue chromophore at 630 nm ascribable to the $Pt(2.25+)_4$ species. Moreover, the compounds have been judged to be diamagnetic, and therefore the $S = {}^1/_2$ spins derived from the $Pt(2.25+)_4$ units must be diamagnetically coupled in the solid state, suggesting that the repeating unit should be expressed as $[Pt(2.25+)_8]_n$ (n is undetermined).

Introduction

Great advances have been made so far in the area of one-dimensional metal chain complexes having infinite metal−metal interactions or bonds.[2] Attractive features exhibited by the linear chain substances are the metallic behaviors as electrical conductors as well as the highly aniosotropic spectroscopic properties. Two well-known families derive from the tetracyanoplatinate and bis(oxalato)platinate systems.[2] In both systems, square-planar platinum coordination planes stack in a *staggered* manner to give 1D platinum chains in the crystal. Their interesting physical properties arise mainly from electron delocalization along the overlapped Pt $5d_{z^2}$ orbitals. Partially oxidized 1D platinum systems (such as $K_2[Pt(CN)_4]\text{-}Br_{0.3}\cdot 3H_2O$), having an average Pt oxidation state of 2.3+ and possessing Pt−Pt bonds of 2.8−3.0 Å, exhibit metallic luster and conductivity, while 1D Pt(II) compounds (such as $K_2[Pt(CN)_4]\cdot 3H_2O$), possessing Pt−Pt bonds of 3.1−3.8 Å (bond order = 0), do not exhibit such attractive properties.[2] Despite the great progress which had been made in the 1970s and the 1980s, the synthetic approach to obtain a new type of linear platinum chain solids has been unsuccessful in recent years. Recent studies in this area rather focus on the spectroscopic properties of 1D platinum(II) chains involving very weak metal−meal bonds.[3−5]

* To whom correspondence should be addressed. E-mail: ksakai@ch.seikei.ac.jp. Fax: +81-422-37-3871.

† Department of Industrial Chemistry, Seikei University.

‡ Department of General Education, Senshu University (SIMS).

§ Department of Applied Physics, Seikei University (XPS).

(1) Part of this study was presented at an international meeting: Sakai, K.; Tsubomura, T.; Ato, M. *30th Int. Conf. Coord. Chem.* (Kyoto) **1994**, S2-57.

(2) (a) Miller, J. S., Ed. *Extended Linear Chain Compounds*; Plenum Press: New York, 1982. (b) Keller, H. J., Ed. *Chemistry and Physics of One-Dimensional Metals*; Plenum Press: New York, 1977. (c) Gliemann, G.; Yersin, H. *Struct. Bonding* **1985**, *62*, 87.

(3) (a) Houlding, V. H.; Miskowski, V. M. *Coord. Chem. Rev.* **1991**, *111*, 145 and references therein. (b) Miskowski, V. M.; Houlding, V. H. *Inorg. Chem.* **1991**, *30*, 4446. (c) Connick, W. B.; Marsh, R. E.; Schaefer, W. P.; Gray, H. B. *Inorg. Chem.* **1997**, *36*, 913. (d) Herber, R. H.; Croft, M.; Coyer, M. J.; Bilash, B.; Sahiner, A. *Inorg. Chem.* **1994**, *33*, 2422 and references therein.

(4) (a) Yip, H. K.; Cheng, L. K.; Cheung, K. K.; Che, C. M. *J. Chem. Soc., Dalton Trans.* **1993**, 2933. (b) Bailey, J. A.; Hill, M. G.; Marsh, R. E.; Miskowski, V. M.; Schaefer, W. P.; Gray, H. B. *Inorg. Chem.* **1995**, *34*, 4591. (c) Hill, M. G.; Bailey, J. A.; Miskowski, V. M.; Gray, H. B. *Inorg. Chem.* **1996**, *35*, 4585.

(5) Palmans, R.; MacQueen, D. B.; Pierpont, C. G.; Frank, A. J. *J. Am. Chem. Soc.* **1996**, *118*, 12647.

10.1021/ja980055p CCC: $15.00
Published on Web 10/27/1998

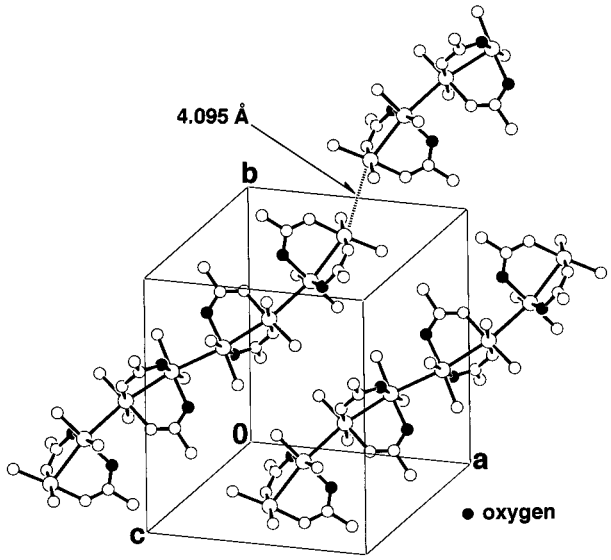

Figure 1. Crystal packing view of octaplatinum cations in $[Pt(2.25+)_2(NH_3)_4(\mu\text{-}CH_3CONH)_2]_4(NO_3)_{10}\cdot 4H_2O$ (drawn with atomic coordinates reported in refs 8a,c), where counterions and solvent water molecules are omitted for clarity.

On the other hand, the syntheses and chemistry of the "platinum blues" have experienced a rapid progress in the last 20 years.[6−8] Although the original interest in this family lay in their intense blue colors, studies on the antitumor activity of *cis*-$Pt(NH_3)_2Cl_2$[9] also stimulated research in this area. This is because the "platinum-pyrimidine blues" obtained from the hydrolysis product of *cis*-$Pt(NH_3)_2Cl_2$ (i.e., *cis*-$[Pt(NH_3)_2(OH_2)_2]^{2+}$) and pyrimidine bases were also found to exhibit high indexes of antitumor activity.[10] Since Barton and Lippard reported on the first X-ray structure of an α-pyridonate blue,[6a] several platinum blues and the related dimers and tetramers at different Pt oxidation levels (2.0+, 2.25+, 2.5+, and 3.0+) have been isolated and structurally characterized.[6−8] The so-called platinum blue cation can be formulated as $[Pt(2.25+)_2(NH_3)_4(\mu\text{-amidato-N,O})_2]_2^{5+}$, in which the tetraplatinum chain structure is formed by a linear stack of two dimeric units doubly bridged with amidate ligands and the formal Pt oxidation state is given by $Pt^{II}_3Pt^{III}$, leading to the expression of $Pt(2.25+)_4$. The platinum blue cation involves similarly short Pt−Pt bonds of about 2.8−2.9 Å and is, therefore, regarded as a partial structure of the partially oxidized 1D platinum chain solids mentioned above.

In this context, we have been endeavoring, over many years, to develop a *1D platinum blue system*. Our first success in this project was achievement of an octaplatinum(2.25+) chain structure using a *sterically free* "acyclic amidate", i.e., acetamidate (see Figure 1).[8] Prior to that study, the platinum blues were generally prepared with use of exocyclic amidate ligands, such as α-pyridonate, α-pyrrolidinonate, 1-methyluracilate, and 1-methylthyminate, and it was assumed that dimeric units constructed with these amidates would never afford either a trimer or oligomers of dimers due to the steric bulks of exocyclic amidate rings covering the N(amidato)-coordinated platinum geometries. Although we failed in achieving a desirable system involving infinite Pt−Pt bonds in the acetamidate system, one important aspect could be drawn out of the picture given in Figure 1, as follows. There are, *unfortunately*, no intermolecular interactions in the crystal due to the long interoctamer Pt−Pt distance of 4.095(2) Å. An important question here is why the dimer−dimer interactions must be disconnected only at this geometry, although the dimer units actually line up in a pseudo-one-dimensional manner and there is no steric bulk at either end of the octamer unit. One may consider that this is just because the octamer unit does not possess any Pt−Pt bonding ability at either end of the unit due to the localization of the partially oxidized nature (i.e., two Pt(III) atoms) over the inner Pt atoms. One may also consider that this is a manifestation of the Peierls' theorem. However, an important feature is that the oxygen atoms of amidates are always present where the interdimer Pt−Pt bonds are formed. In other words, all the dimer−dimer interactions are stabilized not only by a Pt−Pt bond but also by four hydrogen bonds formed with the O(amidate) atoms (this is also true in the classical tetraplatinum blue systems). Thus, we realized that *the hydrogen-bonding interactions may play an important role in stabilizing a dimer−dimer connection*.

Chart 1

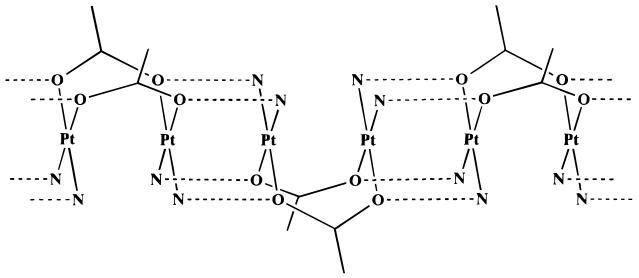

The above concept provided us a very simple idea that carboxylate-bridged dimer compounds may be suited to our purpose. As illustrated in Chart 1, a carboxylate-bridged *cis*-diammineplatinum dimer possesses two oxygen donor ligands at each end of the unit and also possesses two ammine ligands which can be hydrogen-bonded to the oxygen atoms. Such an N_2O_2-coordinated Pt geometry can be, therefore, regarded as a "dimer−dimer connection moiety". We can expect the formation of a hydrogen-bonded chain of dimers as illustrated in Chart 1. The stacking manner in this framework must be distinguished from those in the tetracyanoplatinate system, for the platinum coordination planes would stack in an *eclipsed* fashion. Of course, our final goal is to achieve a partially oxidized system, even though it is, at present, ambiguous whether such a framework leads to a new attractive physical property. However, we believe efforts to develop new materials are themselves important and must be continuously undertaken by chemists.

In the present study, we have confirmed that some carboxylate-bridged dimers indeed give infinite dimer chains through hydrogen-bonding interactions as shown in Chart 1. We report here on the syntheses and crystal structures of some $[Pt_2(NH_3)_4(\mu\text{-carboxylato})_2]^{2+}$ complexes (carboxylato = acetato, glycolato, and benzoato), in which some are 1D and others are not. We also report on 1D frameworks exhibited by two asymmetric

(6) (a) Barton, J. K.; Szalda, D. J.; Rabinowitz, H. N.; Waszczak, J. V.; Lippard, S. J. *J. Am. Chem. Soc.* **1979**, *101*, 1434. (b) O'Halloran, T. V.; Mascharak, P. K.; Williams, I. D.; Roberts, M. M.; Lippard, S. J. *Inorg. Chem.* **1987**, *26*, 1261 and references therein.

(7) Zangrando, E.; Pichierri, F.; Randaccio, L.; Lippert, B. *Coord. Chem. Rev.* **1996**, *156*, 275.

(8) (a) Sakai, K.; Matsumoto, K. *J. Am. Chem. Soc.* **1989**, *111*, 3074. (b) Sakai, K.; Matsumoto, K.; Nishio, K. *Chem. Lett.* **1991**, 1081. (c) Matsumoto, K.; Sakai, K.; Nishio, K.; Tokisue, Y.; Ito, R.; Nishide, T.; Shichi, Y. *J. Am. Chem. Soc.* **1992**, *114*, 8110.

(9) (a) Sherman, S. E.; Lippard, S. J. *Chem. Rev.* **1987**, *87*, 1153. (b) Reedijk, J. *Inorg. Chim. Acta* **1992**, *198*−*200*, 873. (c) Takahara, P. M.; Frederick, C. A.; Lippard, S. J. *J. Am. Chem. Soc.* **1996**, *118*, 12309 and references therein.

(10) (a) Davidson, J. P.; Faber, P. J.; Fischer, R. G., Jr.; Mansy, S.; Peresie, H. J.; Rosenberg, B.; Van Camp, L. *Cancer Chemother. Rep.* **1975**, *59*, 287. (b) Rosenberg, B. *Cancer Chemother. Rep.* **1975**, *59*, 589.

Scheme 1

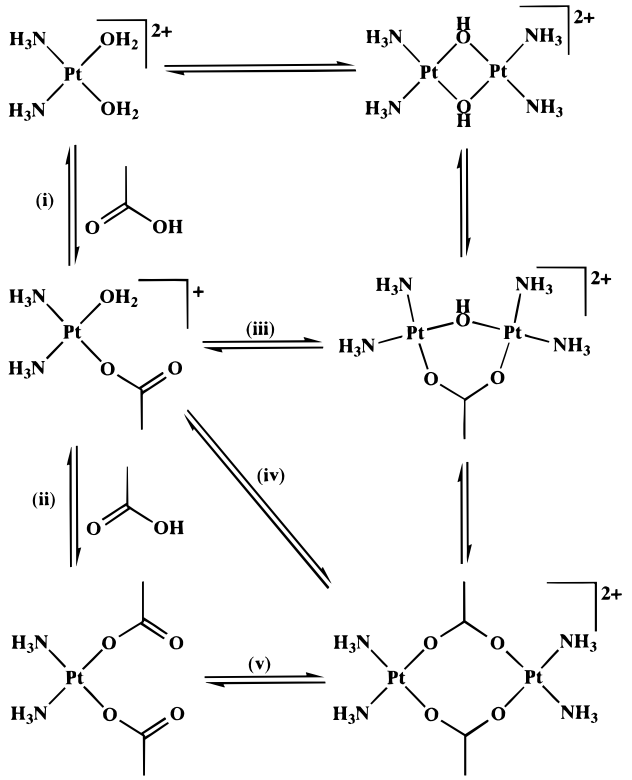

dimers bridged by both carboxylate and hydroxide ligands, $[Pt_2(NH_3)_4(\mu\text{-carboxylato})(\mu\text{-OH})]^{2+}$ (carboxylato = acetato and glycolato). We also report here on a partially oxidized system achieved by using a *p*-hydroxybenzoate ligand.

Results and Discussion

Reactions of *cis*-$[Pt(NH_3)_2(OH_2)_2]^{2+}$ with sodium acetate were once studied by Appleton et al. by means of ^{1}H, ^{15}N, and ^{195}Pt NMR.[11] They showed that (A) a 1:1 reaction between *cis*-$[Pt(NH_3)_2(OH_2)_2]^{2+}$ and sodium acetate rapidly affords a monoacetatoplatinum complex (Scheme 1, i), (B) with a large excess of sodium acetate, a bis(acetato)platinum monomer is yielded as a major product (Scheme 1, ii), and (C) at higher [Pt]/[acetate] ratios ([Pt]/[acetate] > 1), an asymmetric dimer bridged by both acetate and hydroxide ligands, $[Pt_2(NH_3)_4(\mu\text{-}CH_3CO_2)(\mu\text{-OH})]^{2+}$, is given (Scheme 1, iii). From a 1:1 reaction, they also isolated a bright yellow compound having a composition of $Pt(NH_3)_2(CH_3CO_2)(ClO_4)\cdot H_2O$, which was further confirmed by IR to involve bridging acetates. Although they proposed two possible structures, an infinite chain (not shown in Chart 1) and a dimeric unit, for this compound, we assumed that this must be the dimer which we planned to prepare in this study.

To ascertain our assumption, we first measured a secondary ion mass spectrum (SIMS) of the perchlorate salt (see Figure 2). The SIMS displayed parent peaks centered at 675.70 *m*/*z*, which corresponds to a mass unit of $\{[Pt_2(NH_3)_4(\mu\text{-}CH_3CO_2)_2](ClO_4)\}^+$ (675.82). The observed isotope pattern is consistent with the simulated pattern. At this point, we were fully convinced that this compound must be reformulated as $[Pt_2(NH_3)_4(\mu\text{-}CH_3CO_2)_2](ClO_4)_2\cdot 2H_2O$ (**1**), and we therefore started our efforts to grow quality single crystals of this dimer complex. First, we tried to determine the crystal structure of the perchlorate salt which grows as fairly fine filamentous crystals. The samples occasionally involved a quite small amount of well-shaped needles which exhibited effective X-ray diffraction peaks. However, we were not able to determine the appropriate unit cell parameters due to an unavoidable twining problem.

(11) Appleton, T. G.; Berry, R. D.; Davis, C. A.; Hall, J. R.; Kimlin, H. A. *Inorg. Chem.* **1984**, *23*, 3514.

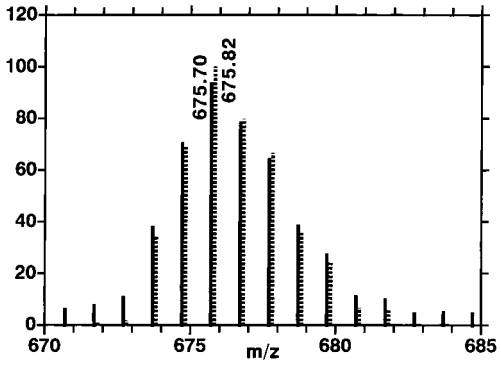

Figure 2. Observed (solid lines) and calculated (dotted lines) isotopic distribution patterns of $\{M - (ClO_4)\cdot 2H_2O\}^+$ for $[Pt_2(NH_3)_4(\mu\text{-}CH_3CO_2)_2](ClO_4)_2\cdot 2H_2O$ (**1**), obtained by SIMS using glycerol as a matrix.

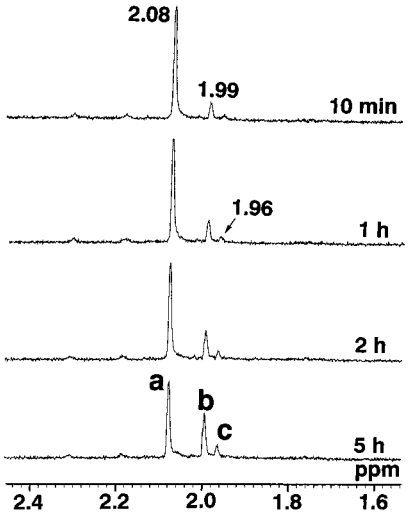

Figure 3. Time course of ^{1}H NMR after dissolution of **2** in D_2O, where signals a−c correspond to $[Pt_2(NH_3)_4(\mu\text{-}CH_3CO_2)_2]^{2+}$, *cis*-$[Pt(NH_3)_2(OCOCH_3)(OH_2)]^+$, and *cis*-$[Pt(NH_3)_2(OCOCH_3)_2]$, respectively. Compounds **1**, **3**, **4**, and **5** showed the same spectral changes.

Therefore, we attempted to prepare several different dimer salts using a variety of counterions: $[Pt_2(NH_3)_4(\mu\text{-}CH_3CO_2)_2](NO_3)_2\cdot H_2O$ (**2**), $[Pt_2(NH_3)_4(\mu\text{-}CH_3CO_2)_2](BF_4)_2\cdot 4H_2O$ (**3**), and $[Pt_2(NH_3)_4(\mu\text{-}CH_3CO_2)_2](PF_6)_2\cdot 2H_2O$ (**4**). In the syntheses of the F-containing salts **3** and **4**, polypropylene vials were used, and reactions were conducted at room temperature in order to avoid both reactions with glassware and decomposition of the anions. Interestingly, **1**−**4** are quite different in color with each other. Particularly, the nitrate salt possesses an amazingly *dark red* color. Nevertheless, all the compounds gave a colorless solution after dissolution in D_2O and showed identical ^{1}H NMR behavior (see Figure 3). The dimer cation (singlet a at 2.08 ppm) gradually decomposes into the mononuclear species, *cis*-$[Pt(NH_3)_2(OCOCH_3)(OH_2)]^+$ (singlet b at 1.99 ppm) and *cis*-$[Pt(NH_3)_2(OCOCH_3)_2]$ (singlet c at 1.96 ppm), where the assignments for b and c are based on the results of Appleton et al.[11] Figure 3 suggests that the major decomposition pathways consist of (iv), (i), and (ii) in Scheme 1, even though a heterolytic cleavage (v) may also be possible. These observations also indicate that a paramagnetic component derived from Pt(III) is not involved in these complexes. Therefore, the dark

red color of the NO_3^- salt, *unfortunately*, does not arise from the partial oxidation at the platinum centers. The origin of this chromophore remains uncertain at the moment.

Despite the above efforts, for a long time, no quality single crystals suitable for the X-ray crystallography were obtained. Most of the above compounds tend to grow as very fine needles. Although the crystals of **2** and **3** grow as *apparently* well-formed, very long crystals, they exhibit no X-ray diffraction at all. So these crystals must be bundles of many extremely fine needles. When we almost gave up, we *accidentally* discovered that somewhat beautiful and huge crystals can be grown when an aqueous solution of *cis*-$[Pt(NH_3)_2(OH_2)_2](BF_4)_2$ is prepared *with heat* using a Pyrex glass vial. It was even possible to grow needles having a length of about 5 mm or more. The crystals grew as either well-formed prisms or needles, but they were ascertained to possess identical unit cell parameters. The formula of this orange compound has been determined as $[Pt_2(NH_3)_4(\mu\text{-}CH_3CO_2)_2](SiF_6)\cdot 4H_2O$ (**5**), based on the elemental analysis, SIMS (Figure S1b), and X-ray diffractometry (vide infra). Possible reactions that take place during the heating of *cis*-$[Pt(NH_3)_2(OH_2)_2](BF_4)_2$ can be roughly represented by the following equilibria:

$$BF_4^- + H_2O \underset{\triangle}{\rightleftharpoons} BF_3 + HF + OH^- \quad (1)$$

$$4HF + SiO_2\ (\text{Pyrex glass}) \rightleftharpoons SiF_4 + 2H_2O \quad (2)$$

$$SiF_4 + 2HF \underset{\triangle}{\rightleftharpoons} SiF_6^{2-} + 2H^+ \quad (3)$$

To further test the presence of SiF_6^{2-}, Na_2SiF_6 was added to a solution containing *cis*-$[Pt(NH_3)_2(OH_2)_2](SO_4)$ and sodium acetate, in which sulfate ion was used because a sulfate salt of the dimer never deposits due to the high solubility in water. Although the sparingly soluble Na_2SiF_6 was merely sunken at the bottom of the vial, the same orange crystals were grown upon leaving the mixture under the same conditions (confirmation done by four-axis X-ray diffractometry). However, the crystals grew with inclusion of Na_2SiF_6. Consequently, the above BF_4 decomposition method, which appears to be somewhat unusual, has turned out to be the best way to grow the crystals of the SiF_6^{2-} salt.

As shown in Figure 4, the crystal of **5** indeed involves the 1D structure proposed in Chart 1. The dimer cation is correlated to the adjacent dimers at both ends of the unit through a crystallographic inversion center. Each dimer−dimer interaction is stabilized, with four hydrogen bonds formed between the ammines and the oxygen atoms of acetates (see Figure 4). Intra- and interdimer Pt−Pt distances, together with other structural features, are summarized in Table 1 and are comparable with those previously reported for some amidate-bridged tetranuclear platinum(II) complexes. The Pt ions both adopt a square-planar geometry. Each Pt atom is shifted out of the best plane defined with four coordinated atoms by 0.07(1) Å toward one another, which is indicative of an attractive interaction between the two Pt atoms. One remarkable feature with regard to the dimeric unit is that the torsional twist about the Pt−Pt vector, ω, between the two Pt coordination planes is obviously smaller than those observed in some amidate systems (see Table 1). The C−O(amidato)−Pt angles generally have a more flexible character than the C−N(amidato)−Pt angles due to the higher bonding affinity between the Pt and the N(amidato) atoms,[12−14] and the low flexibility in the C−N−Pt angle is a predominant factor generating a twist in ω; i.e., some amidate-bridged dimer units need to have a large twist in ω so as to minimize the strain

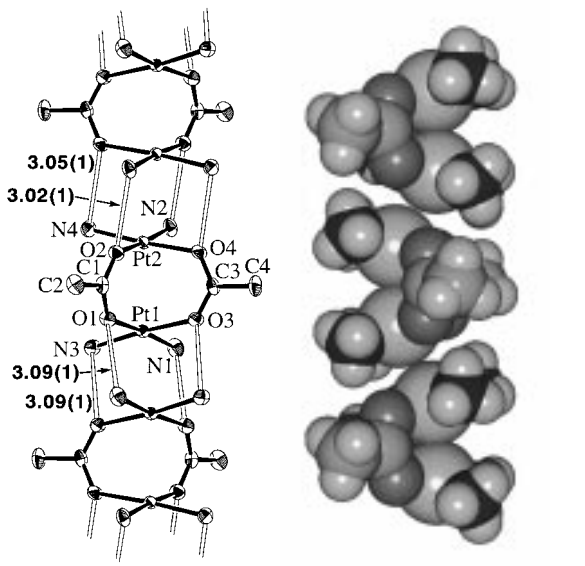

Figure 4. ORTEP view (left, 50% thermal ellipsoids) and space-filling drawing (right) for an infinite dimer chain, $[Pt_2(NH_3)_4(\mu\text{-}CH_3CO_2)_2]_n^{2n+}$, in **5**. Hydrogen bonds for N(ammine)···O(acetate) are drawn with open lines, and the distances (Å) are also depicted.

energy about C−N−Pt.[14] On the other hand, there is no necessity for the acetate-bridged dimer to generate a twist in ω because of the high flexibility in the C−O(acetato)−Pt angle. Although the bite distances of O1···O2 = 2.23(1) and O3···O4 = 2.27(1) Å in the acetate dimer are effectively shorter than the values of 2.3−2.4 Å reported for the amidate-bridged Pt(II) dimers,[12,14] the bridged Pt−Pt distance of the acetate dimer is quite similar to those of the amidate dimers, which also reflects the higher flexibility in C−O(acetato)−Pt. The C−O distances of acetates (1.24(1)−1.28(1) Å) lie in a narrow range, indicating that the double-bond character is equally delocalized over the two C−O units.

Interestingly, the anion−solvent geometry in **5** also exhibits a very attractive 1D framework. As shown in Figure 5, an SiF_6^{2-} anion and four water molecules in the asymmetric unit form a seven-membered macrocycle with relatively strong hydrogen bonds. Moreover, this subunit is strongly hydrogen-bonded to the adjacent subunits to form a 1D chain, $[(SiF_6)(H_2O)_4]_n^{2n-}$. This chain grows in the [111] direction, which is parallel to the direction of the dimer chains. One of the neighboring dimers caps onto the SiF_6^{2-} ion with four hydrogen bonds formed between the ammines and the F(SiF_6^{2-}) atoms, stabilizing the interchain interactions. Therefore, the molecular layer shown in Figure 5 may be regarded as a pseudo-two-dimensional sheet $\{[Pt_2(NH_3)_4(\mu\text{-}CH_3CO_2)_2][(SiF_6)(H_2O)_4]\}_n$. However, this sheet is further hydrogen-bonded to the sheets above and below with five independent hydrogen bonds in the range of 3.00(1)−3.09(1) Å. In summary, hydrogen bonds achieved in the crystal can be classified into three groups: (i) *very strong* hydrogen bonds within $[(SiF_6)(H_2O)_4]_n^{2n-}$, (ii) *middle strength* hydrogen bonds for the interchain associations, and (iii) *relatively weak* hydrogen bonds between the pseudo-sheets. The hydrogen bonds formed within the dimer chain are classified into the weakest group (iii), and it might be possible

(12) (a) Laurent, J.-P.; Lepage, P.; Dahan, F. *J. Am. Chem. Soc.* **1982**, *104*, 7335. (b) Hollis, L. S.; Lippard, S. J. *J. Am. Chem. Soc.* **1983**, *105*, 3494. (c) Matsumoto, K.; Miyamae, H.; Moriyama, H. *Inorg. Chem.* **1989**, *28*, 2959. (d) Lippert, B.; Neugebauer, D.; Raudaschl, G. *Inorg. Chim. Acta* **1983**, *78*, 161.

(13) O'Halloran, T. V.; Lippard, S. J. *Inorg. Chem.* **1989**, *28*, 1289.

(14) Sakai, K.; Tanaka, Y.; Tsuchiya, Y.; Hirata, K.; Tsubomura, T.; Iijima, S.; Bhattacharjee, A., *J. Am. Chem. Soc.* **1998**, *120*, 8366.

Table 1. Comparison of the Structural Features of Carboxylate- and Amidate-Bridged Dinuclar Platinum(II) Complexes

chemical formula	Pt−Pt (intra) distance (Å)	Pt−Pt (inter) distance (Å)	Pt−Pt−Pt angle (deg)	τ^a (deg)	ω^b (deg)	interdimer H-bonds O···N distance (Å)
$[Pt_2(NH_3)_4(\mu\text{-acetato})_2](SiF_6)\cdot 4H_2O$ (**5**)	2.9713(8)	3.176(1)	148.58(2)	36.3(3)	7.2	3.02(1),[c] 3.05(1)[c]
		3.2265(9)	158.16(2)			3.09(1),[c] 3.09(1)[c]
$[Pt_2(NH_3)_4(\mu\text{-glycolato})_2](SiF_6)\cdot 4H_2O$ (**7**)	2.9892(9)	3.2735(9)	150.30(1)	35.7(3)	1.9	3.16(1),[c] 3.16(1)[c]
$[Pt_2(NH_3)_4(\mu\text{-benzoato})_2]_2(SiF_6)(BF_4)_2$-	2.952(1)			32.7(4)	6.6	
$[cis\text{-}Pt(NH_3)_2(\text{benzoato})_2]\cdot 3H_2O$ (**10**)	2.990(1)			35.5(4)	1.7	
$[Pt_2(NH_3)_4(\mu\text{-acetato})(\mu\text{-OH})](SiF_6)$ (**6**)	3.120(2)	3.242(2)	130.92(3)	104.5(7)	0	3.02(3),[c] 3.34(3)[d]
$[Pt_2(NH_3)_4(\mu\text{-glycolato})(\mu\text{-OH})](NO_3)_2$ (**9**)	3.161(1)	3.272(1)	131.84(2)	107.0(4)	0	3.10(2),[c] 3.27(2)[d]
$[Pt_2(NH_3)_4(\mu\text{-1-methylhydantoinato})_2]_2(NO_3)_4\cdot H_2O$[e]	3.131	3.204	160.5	38.6	7.5[i]	3.02,[c,i] 3.03[c,i]
$[Pt_2(NH_3)_4(\mu\text{-}\alpha\text{-pyridonato})_2]_2(NO_3)_4$[f]	2.8767(7)	3.1294(9)	158.40(3)	30.0	20.3	2.95(1),[c] 3.04(1)[c]
$[Pt_2(NH_3)_4(\mu\text{-}\alpha\text{-pyrrolidinonato})_2]_2(PF_6)_3(NO_3)\cdot H_2O$[g]	3.033(2)	3.186(2)	157.85(8)	35.9	1.0[i]	2.98,[c,i] 3.01[c,i]
$[Pt_2(NH_3)_4(\mu\text{-1-methyluracilato})_2](NO_3)_2\cdot H_2O$[h]	2.937(1)			34.1	25.2	

[a] Dihedral cant between the two adjacent platinum coordination planes determined using the BP70 program. [b] Twist angle of the two platinum coordination planes about the Pt−Pt vector. [c] O(carboxylate/amidate)···N(ammine) distances. [d] O(hydroxide)···N(ammine) distances. [e] Reference 12a. [f] Reference 12b. [g] Reference 12c. [h] Reference 12d. [i] Calculated in teXsan.

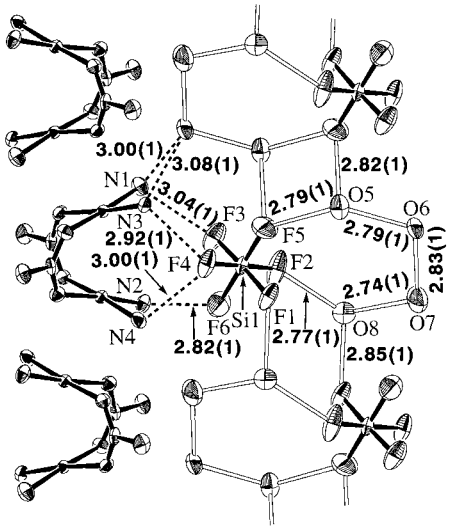

Figure 5. 1D structure of $[(SiF_6)(H_2O)_4]_n^{2n-}$ in the anion and solvent geometry in **5** together with an adjacent $[Pt_2(NH_3)_4(\mu\text{-}CH_3CO_2)_2]_n^{2n+}$ chain, viewed perpendicular to the [111] direction (downward direction). Hydrogen bonds within the anionic chain are drawn with open lines, while those within the cationic chain are omitted for clarity. Interchain hydrogen bonds shorter than 3.10 Å are drawn with dotted lines. The H-bond distances (Å) are also depicted.

that the $[(SiF_6)(H_2O)_4]_n^{2n-}$ framework dominates the crystal packing, leading to the *secondary* achievement of the $[Pt_2(NH_3)_4(\mu\text{-}CH_3CO_2)_2]_n^{2n+}$ framework. However, since the square-planar d^8 metal complexes are known to form stacks with weak metal−metal bonding (M−M = ≈3.2 Å),[2−5] it seems probable that the dimer−dimer associations are stabilized not only by hydrogen bonds but also by weak metal−metal bonds. It is also noteworthy that the same type of hydrogen-bonded dimer chains are achieved even in the absence of the $[(SiF_6)(H_2O)_4]_n^{2n-}$ framework (vide infra). At any rate, our success is that Pt(II) atoms have lined up with a very short average Pt−Pt separation of 3.06 Å (Figure 4). Moreover, it is obvious that a band structure is achieved below the HOMO in this $[Pt_2]_\infty$ chain, since the HOMO of a single dimer unit corresponds to an antibonding couple from the filled−filled d_{z^2}(Pt) orbitals (based on EHMO). Of course, our final goal is to obtain a partially unfilled system leading to a metallic behavior.

After many repeats of the synthesis of **5**, it also became clear that yellow needles codeposit as a byproduct, depending upon the synthetic conditions. This complex has turned out to be an asymmetric dimer bridged by both acetate and hydroxide, $[Pt_2(NH_3)_4(\mu\text{-}CH_3CO_2)(\mu\text{-OH})](SiF_6)$ (**6**). This is a rare example of an asymmetric *cis*-diammineplatinum dimer which is singly bridged by OH and resembles an antitumor-active dimer recently reported by Chikuma et al. ($[Pt_2(NH_3)_4(\mu\text{-pyrazolato})(\mu\text{-OH})](NO_3)_2$).[15] The product yield ratio of **6**/**5** varies from 0 to nearly 1. However, we could not determine a key factor determining the product ratio. Although the pH condition is likely to affect this ratio, no distinct tendency was observed when the pH of the synthetic mixture was adjusted to 4, 5, and 6 prior to the crystallization stage. So, we assume that the product yield ratio is rather controlled by the total equilibria in eqs 1−3, which may vary from batch to batch.

The structure of the dimeric unit in **6** is shown in Figure 6a. A crystallographic mirror passes through the molecule. Because of the structural requirement from the bridging hydroxo ligand, two platinum coordination planes are largely canted at an angle of 104.5(7)°. This value coincides with an average value between 36.3(3)° in **5** and 180° for $[Pt_2(NH_3)_4(\mu\text{-OH})_2]^{2+}$,[16] in agreement with the fact that the dimer in **6** adopts an intermediate structure between them. The bridged Pt−Pt distance of 3.120(2) Å (Table 1) is rather comparable to the values of 3.085(1)[16a] and 3.104(1)[16b] Å reported for $[Pt_2(NH_3)_4(\mu\text{-OH})_2]^{2+}$. The Pt ion nearly adopts a square-planar geometry, but a slight distortion toward T_d is observed (the four-atom rms deviation obtained in the best-plane calculation is 0.077 Å, where a shift of Pt out of this plane is 0.05(1) Å and is meaningless considering the rms deviation of 0.077 Å). As shown in Figure 6b, the crystal of **6** involves a somewhat novel 1D platinum chain. The dimer−dimer associations are stabilized via four hydrogen bonds formed between the ammines and the oxygen atoms of either acetate or hydroxide, quite the same as in **5**. However, in this case, the SiF_6^{2-} ions themselves do not form a chain due to the absence of water molecules. Each SiF_6^{2-} ion is surrounded by six neighboring dimers, and 16 hydrogen bonds in the range of 2.88(2)−3.12(3) Å are formed mainly between the F(SiF_6^{2-}) atoms and the ammines (F···N = 2.88(2)−3.12(3) Å) and also between the F(SiF_6^{2-}) atoms and the hydroxide ions (F···O(OH) = 3.10(3) Å).

Needless to say, the next step is to obtain a partially oxidized blue material having a 1D structure similar to those described above. As observed by many previous platinum blue chemists as well as by Appleton's group,[11] reactions of *cis*-$[Pt(NH_3)_2(OH_2)_2]^{2+}$ with weak oxo-acids, such as acetate and phosphate,

(15) (a) Chikuma, M.; Yamane, H.; Harikawa, M.; Komeda, S.; Yamauchi, T.; Ohishi, H.; Sakaguchi, K. *30th Int. Conf. Coord. Chem.* (Kyoto) **1994**, PS4-77. (b) Chikuma, M.; Hirai, M.; Komeda, S.; Kimura, Y.; Kumakura, K. *J. Inorg. Biochem.* **1997**, *67*, 348.

(16) (a) Faggiani, R.; Lippert, B.; Lock, C. J. L.; Rosenberg, B. *J. Am. Chem. Soc.* **1977**, *99*, 777. (b) Lippert, B.; Lock, C. J. L.; Rosenberg, B.; Zvagulis, M. *Inorg. Chem.* **1978**, *17*, 2971.

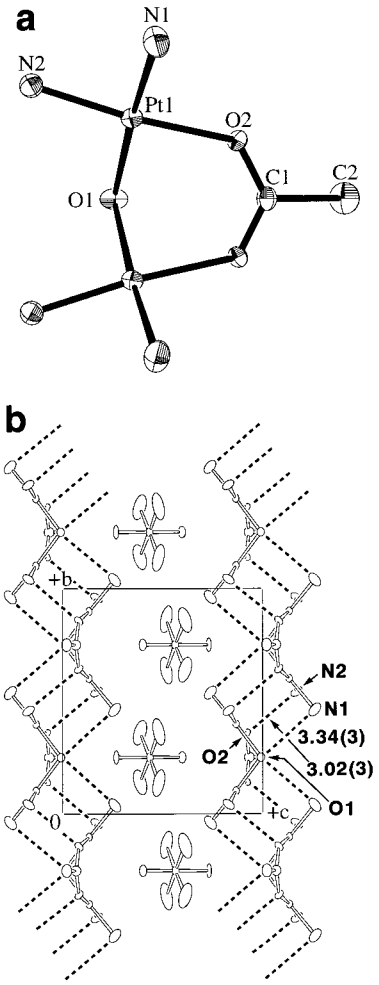

Figure 6. (a) ORTEP view of $[Pt_2(NH_3)_4(\mu\text{-}CH_3CO_2)(\mu\text{-}OH)]^{2+}$ in **6** (50% thermal ellipsoids). (b) 1D structure of $[Pt_2(NH_3)_4(\mu\text{-}CH_3CO_2)(\mu\text{-}OH)]_n^{2n+}$ in **6**, viewed along the *a*-axis, where only the molecules within $-0.25 < a < 0.25$ are extracted. Hydrogen bonds within dimer chains are drawn with dotted lines, in which two independent H-bond distances (Å) are also depicted. Hydrogen bonds between the dimers and the $F(SiF_6^{2-})$ atoms are omitted for clarity.

lead to the formation of paramagnetic blue species. Therefore, it is quite reasonable to expect the formation of an acetate blue. However, after our extensive efforts, we rather became aware of the fact that the oxidation of the acetate dimer into the higher valence states is not so easy because of the relatively high redox potential of the complex ($E_{1/2}(Pt^{II}_2/Pt^{III}_2) = 1.0$ V vs SCE, see Experimental Section for the details). In the case of the acetamidate-bridged dimer $[Pt_2(NH_3)_4(\mu\text{-}CH_3CONH)_2]^{2+}$, the redox potential corresponding to the Pt^{II}_2/Pt^{III}_2 couple levels at 0.42 V vs SCE,[17] and therefore the complex can be easily air-oxidized into the blue species, merely by leaving a solution of the complex in a refrigerator. However, it takes *several month*s to obtain a blue solution in the acetate system. Therefore, we turned our attention to the use of other carboxylates having a stronger donor ability, for it is generally true that a stronger donor ligand gives rise to a lower redox potential at the metal centers. In this context, we expected that benzoate would have a stronger donor ability than acetate owing to the electron-rich character of the phenyl moiety. Indeed, a dark blue precipitate could be more easily obtained with use of benzoate, and the compound displayed a quasi-reversible redox wave at 0.82 V vs SCE. However, we could not obtain a crystalline sample because of its poor crystallizability.

Although we succeeded in obtaining a crystalline benzoate complex having a somewhat complicated formula, $[Pt_2(NH_3)_4(\mu\text{-}C_6H_5CO_2)_2]_2(SiF_6)(BF_4)_2[cis\text{-}Pt(NH_3)_2(C_6H_5CO_2)_2]\cdot 3H_2O$ (**10**), using the BF_4 decomposition method, X-ray structure analysis has shown that the compound does not involve an infinite dimer chain. Despite the pale blue color of **10**, the oxidation state Pt(II) is evident from the crystal structure described below. The net diamagnetic character has also been confirmed both by ^1H NMR using Evans's method[18] and by EPR at room temperature. Although X-ray photoelectron spectra (XPS) were measured to determine the oxidation level of each sample, this physical technique was found to be an inappropriate means to distinguish the pure Pt(II) species from the mixed-valence species (see Table 2). One possibility is that the blue chromophore arises from a certain charge-transfer transition, such as a metal−metal-to-ligand charge-transfer (MMLCT[4,20,21]) transition, $d\sigma^*(Pt\ d_{z^2}) \rightarrow \pi^*$(benzoate). However, our difficulty in evaluating this chromophore lies in that the absorptivity of this chromophore is relatively small, and therefore the oscillation strength for the transition should be very small. As a result, the origin of this chromophore remains unclear at the moment.

As shown in Figure 7a, the asymmetric unit of **10** involves two independent dimer cations and a bis(benzoato)platinum-(II) monomer. The bridged Pt−Pt distances of the dimers are quite comparable to that in **5** (Table 1). The two Pt atoms in each dimer unit have an attractive interaction toward one another in the same manner as in **5** (Pt(1), Pt(2), Pt(4), and Pt-(5) atoms are shifted out the coordination plane by 0.049(7), 0.052(7), 0.061(6), and 0.083(7) Å, respectively, where the four-atom rms deviations in the plane calculations are 0.003−0.018 Å). While the crystal packing of either **5** or **6** is mainly stabilized by electrostatic interactions, both aromatic−aromatic and electrostatic interactions dominate the construction of the crystal of **10**. As shown in Figure 7b, hydrophilic and hydrophobic interactions are separately achieved along the planes defined with $a = 0 \pm n$ and $a = 0.5 \pm n$, respectively. The former involves extensive hydrogen bonds among $F(SiF_6^{2-}/BF_4^-)$ atoms, ammines, and water molecules. The latter involves intermolecular π-stacking interactions between the benzoate ligands (the average plane-to-plane separation is 3.46 Å).

In addition to the above results, very similar 1D frameworks have been characterized using glycolate as a bridging ligand. Although the space group for complex **7** has a higher symmetry than that of **5** (a 2-fold axis passes through the dimer unit), the fundamental construction of the crystal is quite identical to that of **5**. The detailed structural features have been deposited as Supporting Information. The Pt−Pt distances in **7** (Table 1) are slightly longer than those in **5**, reflecting the electron-withdrawing character of the hydroxyl group. This is because the positively charged Pt(II) centers must have a repulsive interaction toward one another, and the positive nature is enhanced by the attachment of OH (we have observed the same phenomena in some new amidate-bridged platinum(II) dimers recently prepared in our laboratory[22]). Note that the bond

(17) Sakai, K.; Kizaki, Y.; Tsubomura, T.; Matsumoto, K. *J. Mol. Catal.* **1993**, *79*, 141.
(18) Evans, D. F. *J. Chem. Soc.* **1959**, 2003.
(19) Barton, J. K.; Best, S. A.; Lippard, S. J.; Walton, R. A. *J. Am. Chem. Soc.* **1978**, *100*, 3785.
(20) (a) Ratilla, E. M. A.; Scott, B. K.; Moxness, M. S.; Kostic, N. M. *Inorg. Chem.* **1990**, *29*, 918. (b) Yip, H. K.; Che, C. M.; Zhou, Z. Y.; Mak, T. C. W. *J. Chem. Soc., Chem. Commun.* **1992**, 1369. (c) Bailey, J. A.; Miskowski, V. M.; Gray, H. B. *Acta Crystallogr.* **1993**, *C49*, 793. (d) Bailey, J. A.; Miskowski, V. M.; Gray, H. B. *Inorg. Chem.* **1993**, *32*, 369.
(21) Cheung, T. C.; Cheung, K. K.; Peng, S. M.; Che, C. M. *J. Chem. Soc., Dalton Trans.* **1996**, 1645.

Table 2. Pt $4f_{7/2}$ and $4f_{5/2}$ Binding Energies

complex	binding energy (eV)[a] Pt $4f_{5/2}$	Pt $4f_{7/2}$	ref
$[Pt(2.0+)_2(NH_3)_4(\mu\text{-acetato})_2](ClO_4)_2\cdot 2H_2O$ (**1**)	76.1 (2.2)	72.8 (2.2)	this work
$[Pt(2.0+)_2(NH_3)_4(\mu\text{-acetato})_2](NO_3)_2\cdot H_2O$ (**2**)	75.7 (2.2)	72.7 (2.2)	this work
$[Pt(2.0+)_2(NH_3)_4(\mu\text{-acetato})_2](SiF_6)\cdot 4H_2O$ (**5**)	76.2 (2.1)	73.1 (2.0)	this work
$[Pt(2.0+)_2(NH_3)_4(\mu\text{-benzoato})_2]_2(SiF_6)(BF_4)_2$-[*cis*-$Pt(2.0+)(NH_3)_2(benzoato)_2]\cdot 3H_2O$ (**10**)	76.4 (1.9)	73.1 (1.9)	this work
$[Pt(2.25+)_2(NH_3)_4(\mu\text{-phbz})_2]_2(SO_4)_{2.25}(phbz)_{0.5}\cdot 5H_2O$ (**12a**)[b]	76.1 (2.0)	72.9 (2.0)	this work
$[Pt(2.25+)_2(NH_3)_4(\mu\text{-}\alpha\text{-pyrrolidinonato})_2]_2(ClO_4)_5$	76.1 (2.0)	72.8 (2.0)	this work
$[Pt(2.25+)_2(NH_3)_4(\mu\text{-}\alpha\text{-pyridonato})_2]_2(NO_3)_5\cdot H_2O$	76.2 (1.5)	72.8 (1.4)	19
$[Pt(2.5+)_2(NH_3)_4(\mu\text{-}\alpha\text{-pyrrolidinonato})_2]_2(NO_3)_6\cdot 2H_2O$	76.4 (2.2)	72.9 (2.1)	this work

[a] Binding energies obtained in this work were all determined by a conventional deconvolution procedure, and values in parentheses correspond to the full width at half-maximum height for each peak. [b] phbz = *p*-hydroxybenzoate.

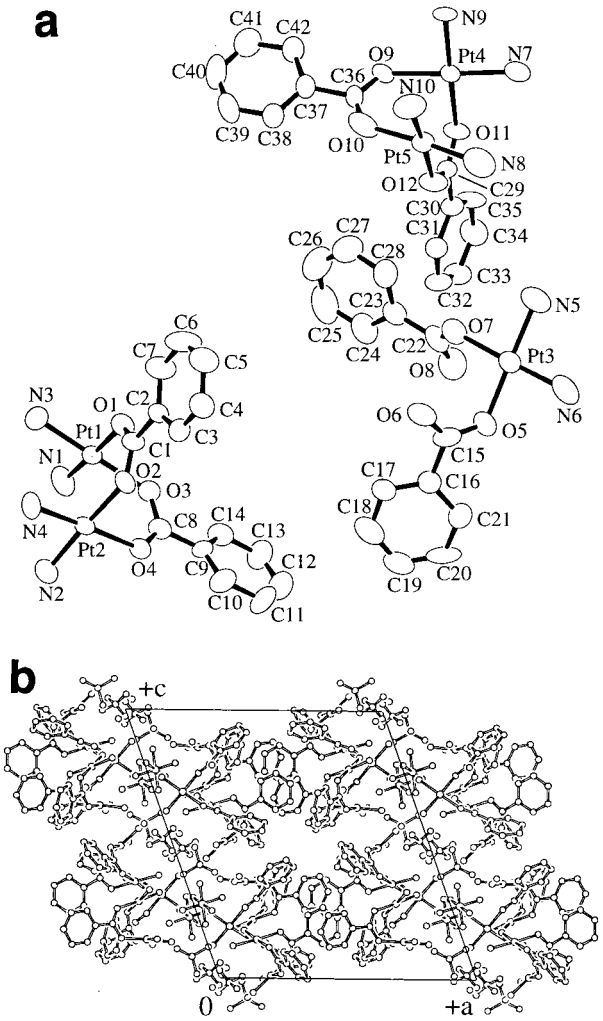

Figure 7. (a) ORTEP view in the asymmetric unit of **10** (50% thermal ellipsoids), where counterions and solvent water molecules are omitted for clarity. (b) Crystal packing view of **10**, down the *b*-axis, within a molecular layer of $-0.5 < b < 0.5$, where atoms are drawn with ideal spheres for clarity.

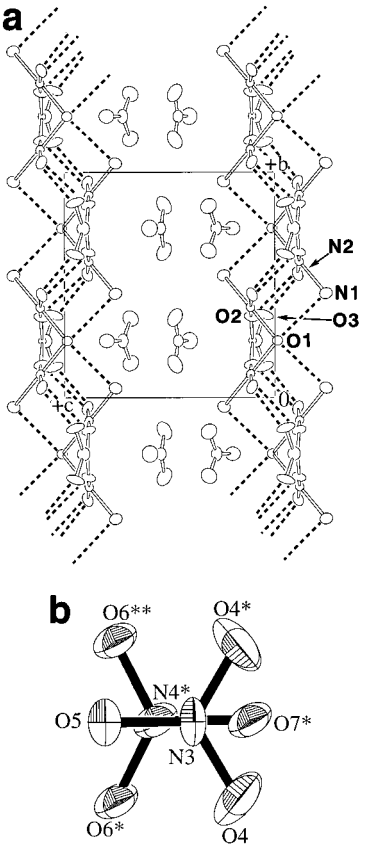

Figure 8. (a) Structure of **9**, viewed along the *a*-axis, where only the molecules within $-0.25 < a < 0.25$ are extracted (50% thermal ellipsoids). Hydrogen bonds within the dimer chains are drawn with dotted lines, where the hydrogen bond distances are O1···N1 = 3.27(2), O2···N2 = 3.10(2), and O3···N2 = 3.07(3) Å. The remaining hydrogen bonds in the crystal are omitted for clarity. (b) View of the $(NO_3)_2^{2-}$ anion perpendicular to the stacked planes. Selected interatomic distances (Å) are as follows: N4*···N3 = 3.27(3); N3···O7* = 3.25(3); O7*···O4 = 3.24(2); N4*···O5 = 3.53(3); O5···O6* = 3.74(2).

lengths of glycolate makes it impossible that the ligand is partly converted into oxalate.

The structure of an asymmetric dimer of glycolate **9** has also been characterized. Interestingly, the space group and the molecular arrangement are quite identical to those in **6**, despite the difference of the counterion (Figure 8a). In **9**, a π-stack dimer of NO_3^- ions, $(NO_3)_2^{2-}$, (Figure 8b), occupies the geometry which is occupied by the SiF_6^{2-} ion in **6**. The shortest internitrate atomic distance is found in O4···O7* = 3.24(2) Å, and the average distance between the two nitrate planes is estimated to be 3.26 Å, which is amazingly short despite the electrostatic repulsion between the two negatively charged molecules. To the best of our knowledge, such strong stacking has never been observed before for the nitrate ion. Although the $(NO_3)_2^{2-}$ unit has a larger molecular volume than has the SiF_6^{2-} ion, the six O(NO_3^-) atoms play a role very similar to

(22) Shiomi, M.; Sakai, K.; Tsubomura, T. *2nd Int. SPACC Symp.* (Tokyo) **1994**, 69. At this meeting, we reported that a head-to-head dimer, $[Pt_2(NH_3)_4(\mu\text{-}N\text{-methylisonicotiamidato})_2]^{4+}$, possesses a very long bridged Pt−Pt distance of 3.05 Å. We think this is responsible for the electron-withdrawing character of the *N*-methylpyridinium moiety. The details of this study will be separately reported elsewhere.

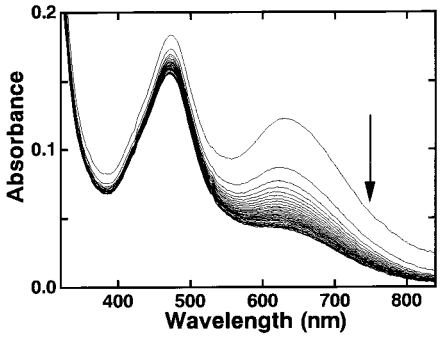

Figure 9. Time course of absorption spectra after dissolution of **12c** in water (3×10^{-5} M) at 25 °C in air, recorded every 1 min. The dead time for the dissolution stage was 4 s, and the time consumed in scanning each spectrum was 33 s.

that of the F(SiF_6^{2-}) atoms. In addition to this feature, the interdimer association in **9** is supported not only by four hydrogen bonds formed between the N_2O_2 coordination spheres, but also by two additional hydrogen bonds formed between the ammines and the oxygen atoms of hydroxyl groups (hydrogen bond lengths are given in Table 1 and Figure 8a). Strictly speaking, the dimer−dimer connection is stabilized with *four to six* hydrogen bonds, since the O(hydroxyl) atom is disordered over two sites, with each site having an occupancy factor of 0.5. Note that this disorder model has been judged to be correct considering the following three facts. First, it was not possible to locate two oxygen atoms each having an occupancy factor of 1.0. Second, the bond distances of C1−C2 = 1.50(3), C1−O2(carboxylate) = 1.24(1), and C2−O3(hydroxyl) = 1.39(2) Å are reasonable for the glycolate ligand. Third, the ligand does not have a planar geometry. These facts make it impossible that the ligand should be treated as an oxalate ion. On the other hand, the intra- and interdimer Pt−Pt distances in **9** are both slightly longer than those in **6** (see Table 1). This is again responsible for the electron-withdrawing character of the hydroxyl unit, as discussed above for **7**.

Since the benzoate system was found to be a favorable one to achieve a partially oxidized system, we further attempted to study a variety of benzoate derivatives, such as *o/m/p*-hydroxybenzoates, dihydroxybenzoates, trihydroxybenzoates, and many others. The hydroxyl group was selected because it favorably promotes water solubility at the phenyl moiety. At the moment, we are paying considerable attention to the *p*-hydroxybenzoate system as one of the most promising candidates. When a solution of *cis*-$[Pt(NH_3)_2(OH_2)_2](ClO_4)_2$ was heated at 70 °C in the presence of an equimolar amount of sodium *p*-hydroxybenzoate, the color of the solution turned to dark blue after only 10 min. Leaving the same starting mixture in a refrigerator overnight afforded a similarly dark blue solution with a dark blue precipitate.

As described in Experimental Section, several *p*-hydroxybenzoate blues whose elemental compositions are unambiguously determined have already been isolated. These compounds are now assumed to have an average platinum oxidation state of 2.25+. Despite their dark blue color, dissolution of them into water immediately affords a red solution, indicating that a quite rapid process takes place in the dissolution stage. As shown in Figure 9, a blue chromophore at 630 nm shows a rapid decay in a triple-exponential image ($k_1 = 0.2$, $k_2 = 0.010(2)$, and $k_3 = 0.00094(9)$ s^{-1}). This implies that Figure 9 covers only the final stage for the first step, even though there still remains large uncertainty about k_1. A decay at 472 nm similarly shows a fit to a triple-exponential curve having the same rate constants, but the extent of decay at this band is relatively small, indicating that both forming and decaying components are involved. On the other hand, only a broad band is observed in the UV region, and it gradually shows a blue shift from 256 to 252 nm as the reaction proceeds. These behaviors, together with the observed rate constants, well resemble those of an α-pyrrolidinonate blue $[Pt(2.25+)_2(NH_3)_4(\mu\text{-}C_4H_6NO)_2]_2(ClO_4)_5$ (674 nm for $Pt(2.25+)_4$ and 478 nm for $Pt(2.5+)_4$; successive right-shifts in $2Pt(2.25+)_4 \rightleftharpoons Pt(2.5+)_4 + 2Pt(2.0+)_2$, $Pt(2.5+)_4 \rightleftharpoons Pt(3.0+)_2 + Pt(2.0+)_2$, and $Pt(2.0+)_2 + O_2 \rightleftharpoons Pt(3.0+)_2$ take place after dissolution).[14] Therefore, a very similar A → B → C mechanism may be postulated for the first two steps: A (presumably $Pt(2.25+)_4$) rapidly gives B (presumably $Pt(2.5+)_4$), but roughly the same amount of B is simultaneously shifted to C (presumably dimers possessing no visible absorption). The slowest step may correspond to the O_2 oxidation process (or to the decomposition in Figure 3). However, further experiments are required in order to clarify the observed phenomena.

Although the X-ray structure determination has not been successful so far, an intriguing finding is that these blue compounds are diamagnetic in the solid state at room temperature (via NMR and EPR). This fact suggests that all the unpaired electrons derived from the $Pt(2.25+)_4$ units ($S = {}^1/_2$) should be diamagnetically coupled in the solid state. Moreover, it is not very likely that the electronic structures of these compounds are similar to that of the acetamidate-bridged $Pt(2.25+)_8$ complex which is diamagnetic, since the acetamidate octamer possesses a metallic, bright red color.[8a,c] Therefore, we have a strong expectation that this is a 1D platinum blue system we intended to prepare in this project.

Concluding Remarks

In this work, we have demonstrated that hydrogen bond formation between the coordinated ligands indeed assists linear stacking of square-planar platinum coordination planes, and suggested that such a secondary factor may become an important synthetic strategy to achieve new 1D metal chain solids. In the present study, we have succeeded in establishing a somewhat unusual but very nice method to grow crystals of SiF_6^{2-} salts. We must emphasize that it would never have been possible to obtain the single crystals analyzed in this study without our finding on the use of SiF_6^{2-}. We have also succeeded, for the first time, in isolating carboxylate-bridged platinum(2.25+) blues which are interestingly *diamagnetic*. Further efforts to achieve one-dimensional platinum blue systems are still in progress in our laboratory.

Experimental Section

Chemicals. *cis*-$Pt(NH_3)_2Cl_2$ (N. E. Chemcat) was used as received. All other reagents were purchased in the highest quality and were used without further purification. $[Pt(2.25+)_2(NH_3)_4(\mu\text{-}\alpha\text{-pyrrolidinonato})_2]_2(ClO_4)_5$ was prepared as described elsewhere.[14] $[Pt(2.5+)_2(NH_3)_4(\mu\text{-}\alpha\text{-pyrrolidinonato})_2]_2(NO_3)_6{\cdot}2H_2O$ was prepared as previously described.[23]

Aqueous Solutions of *cis*-$[Pt(NH_3)_2(OH_2)_2]X_2$ (X = ClO_4^- and NO_3^-, or $X_2 = SO_4^{2-}$). These were prepared according to the conventional method[24] with minor modification as follows. A suspension of *cis*-$Pt(NH_3)_2Cl_2$ (1 mmol, 0.300 g) and AgX (2 mmol) or Ag_2X (1 mmol) in 7−20 mL of water, sealed in a Pyrex screw-cap vial, was stirred at 60 °C for 3 h in the dark, and the AgCl precipitated was removed by filtration.

(23) Sakai, K.; Tsubomura, T.; Matsumoto, K. *Inorg. Chim. Acta* **1993**, *213*, 11.
(24) Lim, M. C.; Martin, R. B. *J. Inorg. Nucl. Chem.* **1976**, *38*, 1911.

Aqueous Solutions of *cis*-$[Pt(NH_3)_2(OH_2)_2]X_2$ (X = BF_4^-, and PF_6^-). To avoid decomposition reactions of BF_4^- and PF_6^-, a suspension of *cis*-$Pt(NH_3)_2Cl_2$ (1 mmol, 0.300 g) and AgX (2 mmol) in 7−20 mL of water was stirred at room temperature for 1 day; a polypropylene vial was also used to avoid chemical reactions with SiO_2 derived from glassware. The AgCl precipitated was removed by filtration.

An Aqueous Solution of *cis*-$[Pt(NH_3)_2(OH_2)_2]^{2+}$ Containing Both BF_4^- and SiF_6^{2-}. This was prepared through decomposition reactions of BF_4^- with SiO_2. A suspension of *cis*-$Pt(NH_3)_2Cl_2$ (1 mmol, 0.300 g) and $AgBF_4$ (2 mmol) in 7 mL of water was sealed in a Pyrex screw-cap vial and was stirred at 70 °C for 3 h in the dark. (*Note: A relatively large-volume vial must be used to gain a large surface area for the reaction between BF_4^- and SiO_2. We typically used a 20-mL vial for a reaction mixture having a volume of 2.33 mL. It is also useful to add some glass beads to the reaction mixture.*) After the mixture was cooled, the gas phase above the solution was replaced with air to remove some harmful gases, such as HF, BF_3, SiF_4, etc. (***Caution!*** *This procedure should be performed in a draft chamber.*) The solution was then filtered to remove the AgCl that precipitated.

Syntheses. $[Pt_2(NH_3)_4(\mu\text{-}CH_3CO_2)_2](ClO_4)_2\cdot 2H_2O$ (1). This was prepared according to Appleton's method[11] with minor modification as follows. To an aqueous solution of *cis*-$[Pt(NH_3)_2(OH_2)_2](ClO_4)_2$ (1 mmol/7 mL) was added $CH_3CO_2H\cdot 3H_2O$ (1 mmol, 0.136 g). Leaving of the solution at 5 °C for 3−4 days afforded the product as bright yellow filaments. Crystals were collected by filtration and were air-dried. Further leaving of the filtrate afforded the same product. Anal. Calcd for $Pt_2Cl_2O_{14}N_4C_4H_{22}$: C, 5.92; H, 2.73; N, 6.91. Found: C, 5.74; H, 2.60; N, 7.03. ***Caution!*** *Although we have experienced no difficulties with the perchlorate salts described in this paper, the compounds should be regarded as potentially explosive and handled with care.*

$[Pt_2(NH_3)_4(\mu\text{-}CH_3CO_2)_2](NO_3)_2\cdot H_2O$ (2). This was prepared in the same manner as **1**, except that *cis*-$[Pt(NH_3)_2(OH_2)_2](NO_3)_2$ (1 mmol/7 mL) was used. Black fine needles were obtained. Anal. Calcd for $Pt_2O_{11}N_6C_4H_{20}$: C, 6.69; H, 2.81; N, 11.70. Found: C, 6.85; H, 2.56; N, 11.63. SIMS (glycerol as matrix): 638.4 *m/z*, $[M - (NO_3)\cdot H_2O]^+$ (Figure S1a).

$[Pt_2(NH_3)_4(\mu\text{-}CH_3CO_2)_2](BF_4)_2\cdot 4H_2O$ (3). This was prepared in the same manner as **1**, except that *cis*-$[Pt(NH_3)_2(OH_2)_2](BF_4)_2$ (1 mmol/7 mL) in a polyethylene vial was used. Slightly greenish yellow needles were obtained. Anal. Calcd for $Pt_2F_8O_8N_4C_4B_2H_{26}$: C, 5.84; H, 3.19; N, 6.82. Found: C, 6.11; H, 3.29; N, 6.84.

$[Pt_2(NH_3)_4(\mu\text{-}CH_3CO_2)_2](PF_6)_2\cdot 2H_2O$ (4). This was prepared in the same manner as **1**, except that *cis*-$[Pt(NH_3)_2(OH_2)_2](PF_6)_2$ (1 mmol/7 mL) in a polyethylene vial was used. Yellow needles were obtained. Anal. Calcd for $Pt_2P_2F_{12}O_6N_4C_4H_{22}$: C, 5.32; H, 2.46; N, 6.21. Found: C, 5.47; H, 2.12; N, 6.20.

$[Pt_2(NH_3)_4(\mu\text{-}CH_3CO_2)_2](SiF_6)\cdot 4H_2O$ (5). This was prepared in the same manner as **1**, except that *cis*-$[Pt(NH_3)_2(OH_2)_2]^{2+}$ involving SiF_6^{2-}/BF_4^- (1 mmol/7 mL) in a Pyrex vial was used. After being left at 5 °C overnight, the solution was filtered to remove a white powder of Na_2SiF_6, whose solubility in water is extremely low. Standing of the solution in the same condition for 3−4 days afforded the product as well-formed orange prisms or needles (yield 20−24%). Crystals were collected by filtration and air-dried. The crystals were manually separated from a side product (**6**) under a microscope (this procedure is not so hard owing to the large size of the crystals). Anal. Calcd for $Pt_2SiF_6O_8N_4C_4H_{26}$: C, 6.08; H, 3.32; N, 7.09. Found: C, 6.21; H, 3.23; N, 7.13.

When acetic acid was used instead of sodium acetate, the identical crystals could be obtained. Although it took a longer period to grow crystals, merits of using the acid form are that the product was never contaminated with Na_2SiF_6 and that quite huge single crystals could be grown.

$[Pt_2(NH_3)_4(\mu\text{-}CH_3CO_2)(\mu\text{-}OH)](SiF_6)$ (6). This was obtained as a side product of **5**, as mentioned above, as yellow needles. Anal. Calcd for $Pt_2SiF_6O_3N_4C_2H_{16}$: C, 3.55; H, 2.38; N, 8.28. Found: C, 3.64; H, 2.65; N, 8.29. The amount of **6** was usually about one-tenth of the amount of **5**. However, sometimes **6** did not appear, and sometimes the yield of **6** was as high as that of **5**. Although we tried to clarify the pH dependence of the yield, no distinct tendency could be observed. As a result, the optimization of the synthetic method is not successful.

$[Pt_2(NH_3)_4(\mu\text{-}CH_2(OH)CO_2)_2](SiF_6)\cdot 4H_2O$ (7). This was prepared in the same manner as **5**, except that either sodium glycolate (1.0 mmol, 0.098 g) or glycolic acid (1.0 mmol, 0.11 g of an aqueous 70% solution) was added instead of sodium acetate. When the sodium form was used, leaving the solution at 5 °C for a few days resulted in deposition of yellow prisms (yield 20%). On the other hand, it took more than a week to grow the crystals when the acid form was used. Anal. Calcd for $Pt_2SiF_6O_{10}N_4C_4H_{26}$: C, 5.84; H, 3.19; N, 6.81. Found: C, 5.92; H, 3.04; N, 6.91. The crystals were apparently homogeneous, and the asymmetric dimer salt did not codeposit. Note that this material is labile upon exposure in air, and the crystals gradually change into a greenish color.

$[Pt_2(NH_3)_4(\mu\text{-}CH_2(OH)CO_2)_2](ClO_4)_2\cdot H_2O$ (8). This was prepared in the same manner as **1**, except that sodium glycolate (1.0 mmol, 0.098 g) was added instead of sodium acetate. The product formed as yellow prisms. Anal. Calcd for $Pt_2Cl_2O_{15}N_4C_4H_{20}$: C, 5.82; H, 2.44; N, 6.79. Found: C, 5.85; H, 2.42; N, 6.82.

$[Pt_2(NH_3)_4(\mu\text{-}CH_2(OH)CO_2)(\mu\text{-}OH)](NO_3)_2$ (9). This was prepared in the same manner as **2**, except that sodium glycolate (1.0 mmol, 0.098 g) was used instead of sodium acetate and it took 3 weeks to grow the yellow prisms of the product (yield 15%). Anal. Calcd for $Pt_2O_{10}N_6C_2H_{16}$: C, 3.56; H, 2.39; N, 12.46. Found: C, 3.71; H, 2.35; N, 12.42.

$[Pt_2(NH_3)_4(\mu\text{-}C_6H_5CO_2)_2]_2(SiF_6)(BF_4)_2[cis\text{-}Pt(NH_3)_2(C_6H_5CO_2)_2]\cdot 3H_2O$ (10). This was obtained in the same manner as **5** with minor modifications as follows. The volume of water added was 9 mL. After the removal of AgCl, sodium benzoate (1 mmol, 0.144 g) was added to the filtrate. After the solution was stirred at room temperature for 3 h, insoluble materials, presumably undissolved sodium benzoate and *cis*-$[Pt(NH_3)_2(C_6H_5CO_2)_2]$ (ca. 0.13 g), were removed by filtration. The solution was allowed to stand at room temperature for 12 h to afford pale blue needles (yield ∼10%). Anal. Calcd for $Pt_5SiF_{14}O_{15}N_{10}C_{42}B_2H_{66}$: C, 22.50; H, 2.97; N, 6.25. Found: C, 21.88; H, 2.91; N, 6.00. The crystals possess an intriguing anisotropic property, i.e., they are colorless when looked at from one face but blue from another face.

***cis*-$[Pt(NH_3)_2(C_6H_5CO_2)_2]\cdot 2H_2O$ (11).** To an aqueous solution of *cis*-$[Pt(NH_3)_2(OH_2)_2]X_2$ (X_2 = $(NO_3)_2$ or SO_4) (1 mmol/20 mL) was added a solution of $C_6H_5CO_2Na$ (10.5 mmol, 1.5 g) in water (1 mL). The white (or very pale yellow) solid precipitated within 10 min was collected by filtration and dried in vacuo (yield 66%). Anal. Calcd for $PtO_6N_2C_{14}H_{20}$: C, 33.14; H, 3.97; N, 5.52. Found: C, 33.23; H, 3.66; N, 5.59. Note that a prolonged reaction results in contamination of the product with pale blue materials. This complex has been used as a sort of complex ligand to prepare dinuclear or multinuclear complexes, but this approach has been unsuccessful so far.

$[Pt(2.25+)_2(NH_3)_4(\mu\text{-}p\text{-}C_6H_4(OH)CO_2)_2]_2X_5\cdot nH_2O$ (X_5, n = $(SO_4)_{2.25}$-$(p\text{-}C_6H_4(OH)CO_2)_{0.5}$, 5, 12a; $(PF_6)_2(SO_4)(p\text{-}C_6H_4(OH)CO_2)$, 6, 12b; $(PF_6)_2(NO_3)_2(p\text{-}C_6H_4(OH)CO_2)$, 7, 12c). For **12a**, to an aqueous solution of *cis*-$[Pt(NH_3)_2(OH_2)_2](SO_4)$ (0.2 mmol/2 mL) was added sodium p-hydroxybenzoate (0.2 mmol, 0.032 g). Standing of the solution for 1−2 weeks afforded the product as dark blue microcrystals (Yield, 5%). Anal. Calcd for $Pt_4S_{2.25}O_{27.5}N_8C_{31.5}H_{56.5}$ (**12a**): C, 20.56; H, 3.10; N, 6.09. Found: C, 20.57; H, 3.08; N, 5.83. **12b** was prepared in the same manner as **12a**, except that KPF_6 (0.2 mmol, 0.037 g) was also added to the mixture (yield 5%). Anal. Calcd for $Pt_4SP_2F_{12}O_{25}N_8C_{35}H_{61}$ (**12b**): C, 20.05; H, 2.93; N, 5.35. Found: C, 20.01; H, 3.17; N, 5.51. **12c** was prepared in the same manner as **12b**, except that *cis*-$[Pt(NH_3)_2(OH_2)_2](NO_3)_2$ was used instead of the sulfate salt (yield 2%). Anal. Calcd for $Pt_4P_2F_{12}O_{28}N_{10}C_{35}H_{63}$ (**12c**): C, 19.62; H, 2.96; N, 6.54. Found: C, 19.34; H, 2.73; N, 6.84.

X-ray Crystallography. All the crystals were mounted on a glass fiber. Diffraction data at 296 K were measured on a Rigaku AFC-5S diffractometer. Graphite-monochromated Mo Kα (0.710 69 Å) radiation was used for **5**, **6**, **7**, and **9**. Only in the structure determination of **10**, a data set collected using graphite-monochromated Cu Kα (1.541 78 Å) radiation was adopted. All the measurements were performed using the $\omega-2\theta$ scan technique (8 deg/min). The unit cell

Table 3. Crystallographic Data

	5	**6**	**7**	**9**	**10**
formula	$Pt_2SiF_6O_8N_4C_4H_{26}$	$Pt_2SiF_6O_3N_4C_2H_{16}$	$Pt_2SiF_6O_{10}N_4C_4H_{26}$	$Pt_2O_{10}N_6C_2H_{16}$	$Pt_5SiF_{14}O_{15}N_{10}C_{42}B_2H_{66}$
fw	790.53	676.43	822.53	674.36	2242.18
cryst color, habit	orange, prism	yellow, prism	green, prism	pale yellow, prism	pale blue, needle
cryst size, mm	0.40 × 0.40 × 0.20	0.43 × 0.23 × 0.13	0.45 × 0.13 × 0.08	0.25 × 0.23 × 0.18	0.83 × 0.13 × 0.05
cryst system	triclinic	orthorhombic	monoclinic	orthorhombic	monoclinic
space group	$P\bar{1}$	*Pnma*	*C*2/*c*	*Pnma*	$P2_1/c$
a, Å	10.313(1)	12.819(2)	14.498(2)	12.689(2)	19.078(4)
b, Å	11.260(2)	10.487(2)	15.401(2)	10.687(3)	17.014(3)
c, Å	10.102(2)	9.253(2)	10.482(2)	9.939(2)	21.212(2)
α, deg	115.48(1)	90	90	90	90
β, deg	93.80(1)	90	127.250(6)	90	109.84(1)
γ, deg	112.16(1)	90	90	90	90
V, Å^3	943.4(3)	1243.9(4)	1863.0(5)	1347.8(5)	6477(1)
Z	2	4	4	4	4
D_{calcd}, g/cm^3	2.7829	3.6119	2.9325	3.3233	2.2995
μ, cm^{-1}	149.71	226.47	151.76	207.97	208.22
F(000)	732.00	1216.00	1528.00	1224.00	4192.00
$2\theta_{max}$ (*hkl* range)	55° (*h*,±*k*,±*l*)	60° (*h*,*k*,*l*)	60° (*h*,*k*,±*l*)	60° (*h*,*k*,*l*)	120° (*h*,*k*,±*l*)
trans coeff[a]	0.4696−1.0000	0.2140−1.0000	0.5155−1.0000	0.5549−1.0000	0.2810−1.0000
decay, %	−0.19 (not corrected)	0 (not corrected)	0 (not corrected)	−0.50 (not corrected)	−0.31 (not corrected)
extinction coeff	9.8(4) × 10^{-7}	2.2(3) × 10^{-7}	0.13(10) × 10^{-7}	5.2(2) × 10^{-7}	0.67(4) × 10^{-7}
no. of reflns measd	5789	2140	2911	2318	10362
no. of unique reflns	5505	2089	2813	2261	10023
no. of reflns used[b]	3587	1003	1841	1373	7949
no. of params	227	92	133	107	785
p factor[c]	0.013	0.013	0.020	0.013	0.010
goodness of fit[d]	2.17	2.85	1.64	2.02	2.43
R^e(R_w^f)	0.0395 (0.0375)	0.0612 (0.0552)	0.0442 (0.0394)	0.0561 (0.0450)	0.0561 (0.0501)

[a] Ψ-scans. [b] $I > 2\sigma(I)$. [c] Weighting scheme is given by $1/w = \sigma^2(F_o) + p^2|F_o|^2$. [d] Goodness of fit $= [\sum w(|F_o| - |F_c|)^2/(n_o - n_p)]^{1/2}$, where n_o = no. of reflns used, and n_p = no. of params. [e] $R = \sum||F_o| - |F_c||/\sum|F_o|$. [f] $R_w = [\sum w(|F_o| - |F_c|)^2/\sum w|F_o|^2]^{1/2}$.

parameters were determined from a least-squares fit of 25 carefully centered reflections (34° < 2*θ* < 35° for **5**; 31° < 2*θ* < 35° for **6**; 33° < 2*θ* < 35° for **7**; 31° < 2*θ* < 35° for **9**; 67° < 2*θ* < 70° for **10**). The space groups for **6**, **7**, **9**, and **10** were uniquely determined by the systematic absences in the final data sets. Crystal and experimental data are summarized in Table 3. All data sets were corrected for Lorentz and polarization effects, and for absorption by employing Ψ scans on three reflections with *χ* near 90°.[25] Metal atom positions were determined by the direct methods (SAPI91[26] for **5**, **6**, **9**, and **10**; SIR88[27] for **7**). Typically, most of the remaining non-hydrogen atoms were located using the DIRDIF[28] program. Complete location of atoms in the final stage of refinements was conventionally done using the difference Fourier technique. All non-hydrogen atoms, except for two $B(BF_4^-)$ atoms in **10**, were refined anisotropically by full-matrix least squares on the teXsan[29] software. Since the refinements of these $B(BF_4^-)$ atoms were not successful, even when they were treated isotropically, they were merely located at a peak position in the difference Fourier map and were not refined. The O(hydroxyl group of glycolate) atoms in **7** and **9** were found to be disordered over two sites that are correlated with either a mirror or a 2-fold axis, and therefore their occupancy factors were set to be 0.5. All hydrogen atoms, except for those of water molecules, hydroxide ligands, and hydroxyl groups, were located in their idealized positions (C−H = 0.95 and N−H = 0.87 Å) and were not refined. The best-plane calculations were performed by using the BP70[30] program. Scattering factors used are those in the literature.[31] The final maximum shift/esd values are 0.0024 (**5**), 0.005 (**6**), 0.007 (**7**), 0.001 (**9**), and 0.009 (**10**). In all the cases, the maximum and minimum peaks in the final difference Fourier maps were relatively large: +2.2 and −2.8 (**5**); +4.8 and −6.9 (**6**); +1.4 and −1.2 (**7**); +3.8 and −3.1 (**9**); +3.3 and −2.2 e/Å^3 (**10**). However, most of these peaks were located near the Pt atoms, and the rest of them were located near the Si and F atoms, and no more atoms could be further located.

Measurements. Secondary ion mass spectra (SIMS) were acquired on a Hitachi M80B mass spectrometer, using glycerol as a matrix. ^{1}H NMR spectra in D_2O were acquired on a JEOL JNM-GX270 spectrometer, in which sodium 2,2-dimethyl-2-silapentane-5-sulfonate (DSS) was used as an internal standard. Cyclic voltammograms were measured on a Huso setup (HECS 321B and 311B). A Pt disk (BAS), a saturated calomel electrode (SCE) (BAS), and a Pt wire were used as the working, the reference, and the counter electrodes, respectively. A solution of 0.1 M tetra(*n*-butyl)ammonium perchlorate (TBAP) in dry acetonitrile was used in each measurement, where the SCE was separated from the electrolysis compartment using a Vycor disk (BAS). Qualitative aspects with regard to the diamagnetic character of the complexes were obtained by ^{1}H NMR using the concept of Evans.[18] In each measurement, a capillary tube having an inner diameter of 1 mm was inserted into a normal 5-mm NMR tube. A $CDCl_3$ solution containing 2% of tetramethylsilane (TMS) was added to both the inner and the outer tubes. A finely ground solid sample was added to the inner tube, where the solid was partly dispersed and partly deposited at the bottom, and the bottom of the inner capillary was positioned within the detectable region. With this method, an effective splitting was observable in the TMS signal when a standard paramagnetic sample, such as $NiSO_4{\cdot}7H_2O$ ($S = 1$) and $[Pt(2.25+)_2(NH_3)_4(\mu\text{-}\alpha\text{-pyrrolidinonato})_2]_2(ClO_4)_5$ ($S = {}^1/_2$),[14] was added. The diamagnetic characters of **10** and **12** were confirmed on a JEOL JES-RE2X EPR spectrometer. X-ray photoelectron spectra were measured on a PHI model 1600 spectrometer at ultrahigh-vacuum pressure less than 5 × 10^{-8} Pa in the analysis chamber. A standard Mg Kα excitation ($h\nu$ = 1253.6 eV) source was used in the measurements. All the samples were placed on an indium plate. The binding energies were standardized with Au ($3d_{5/2}$, 4443.8 eV) spattered on each sample. The accuracy in binding energy is less than 0.1 eV. Visible absorption spectra were

(25) North, A. C. T.; Phillips, D. C.; Mathews, F. S. *Acta Crystallogr.* **1968**, *A24*, 351.
(26) SAPI91: Fan, H. F. *Structure Analysis Programs with Intelligent Control*; Rigaku Corp.: Tokyo, Japan, 1991.
(27) SIR88: Burla, M. C.; Camalli, M.; Cascarano, G.; Giacovazzo, C.; Polidori, G.; Spagna, R.; Viterbo, D. *J. Appl. Crystallogr.* **1989**, *22*, 389.
(28) DIRDIF: Parthasarathi, V.; Beurskens, P. T.; Slot, H. J. B. *Acta Crystallogr.* **1983**, *A39*, 860.
(29) teXsan: *Single-Crystal Structure Analysis Software*, Version 1.6f, 1994. Molecular Structure Corp., 3200 Research Forest Dr., The Woodlands, TX 77381.
(30) BP70: Ito, T. *Acta Crystallogr.* **1982**, *A38*, 869.
(31) Cromer, D. T.; Waber, J. T. In *International Tables for X-ray Crystallography, Vol. IV*; Kynoch Press: 1969; Birmingham, Table 2.2A, pp 71−98.

recorded on a Shimadzu UV-2100S spectrophotometer. The experimental setup used to perform quick dissolution of a solid is reported elsewhere.[14]

Acknowledgment. This work was partly supported by Grants-in-Aid for Scientific Research (Nos. 04854061, 05854065, 06854041, 07854043) from the Ministry of Education, Science, and Culture of Japan. K.S. thanks Dr. Dean A. Katahira (Ripon College, USA) for his helpful discussions at the 30th ICCC meeting site. We thank Dr. Hiroshi Moriyama (Toho University) for the electric conductivity measurement on **5** which confirmed the sample to be an insulator. We thank Professor Kazuko Matsumoto (Waseda University) for the kind use of her EPR facility. We thank Dr. Jiro Abe (Tokyo Institute of Polytechnics) for his kind assistance and helpful discussions with regard to our efforts to characterize the blue chromophore of **10** with *ab initio* MO calculations.

Supporting Information Available: Observed and calculated isotopic distribution patterns (SIMS) for **2** and **5** (Figure S1), and tables of atomic coordinates including hydrogen atom coordinates, anisotropic thermal parameters, and interatomic distances and angles (Table S1-15) (18 pages, print/PDF). X-ray crystallographic files, in CIF format, for **5**-**7**, **9**, and **10** are available on the Web only. See any current masthead page for ordering information and Web access instructions.

JA980055P